Songklanakarin J. Sci. Technol.
30 (3), 323-332, May - Jun. 2008

Songklanakarin Journal of Science and Technology
http://www.sjst.psu.ac.th

Original Article

Cyclic behavior of non-seismically designed interior reinforced concrete beam-column connections

Amorn Pimanmas[1] and Teeraphot Supaviriyakit[2]*

[1]*School of Civil Engineering and Technology, Sirindhorn International Institute of Technology, Thammasat University, Khlong Luang, Pathum Thani, 12121 Thailand.*

[2]*School of Civil Engineering, Naresuan University, Phayao Campus, Mueang, Phayao, Thailand*

Received 7 March 2007; Accepted 23 April 2008

Abstract

This paper presents a test of non-seismically detailed reinforced concrete beam-column connections under reversed cyclic load. The tested specimens represented those of the actual mid-rise reinforced concrete frame buildings, designed according to the non-seismic provisions of the ACI building code. The evaluation of 10 existing reinforced concrete frames was conducted to identify key structural and geometrical indices. It was found that there existed correlation VS structural and geometrical characteristics and the column tributary area. Hence, the column tributary area was chosen as a parameter for classifying the specimens. The test results showed that specimens representing small and medium column tributary area failed by brittle joint shear, while specimen representing large column tributary area failed by ductile flexure, even though no ductile seismic details were provided.

Key words: substandard beam-column joint, reversed cyclic load, joint shear failure, bond deterioration, column tributary area

1. Introduction

The seismic vulnerability of old existing reinforced concrete buildings constructed in zones of low to medium seismicity was recently discussed by several researchers in the USA and New Zealand (Aycardi *et al.*, 1994, Bracci *et al.*, 1995, El-attar *et al.*, 1997, Hakuto *et al.*, 2000). Even in the South East Asian region such as Thailand, Singapore and Malaysia, which was usually believed to be safe against seismic hazard, the research in this issue has gained more attention (Li *et al.*, 2002, Li and Pan, 2004, Warnichai, 2004) due to several recent earthquake occurrences in the region. Most recently the 2004 Sumatra Earthquake in the Andaman Sea, recorded at 9.3 moment magnitude, caused violent shaking of many buildings in Bangkok, though the epicenter was more than 800 kilometers away. The quake has prompted a serious public concern on seismic safety of buildings. In the Southeast Asian countries, there are many low-rise and mid-rise buildings of up to 10 stories constructed as beam-column rigid frames without shear walls. The frame structures mainly resist lateral forces through bending of beams and columns. Most of these structures were designed for gravity load only according to the American Concrete Institute's (ACI) building code in Thailand and British Standard (BC) code in Singapore and Malaysia.

As a result of the lack of seismic consideration in structural design, the reinforcement details of these frame buildings were usually weak against earthquake loading. The beam-column joint is one of the most critical components in the seismic load path. Under lateral force, the joint has to carry a large horizontal shear force (Figure 1) in order to

*Corresponding author.
Email address: teeraphot@hotmail.com

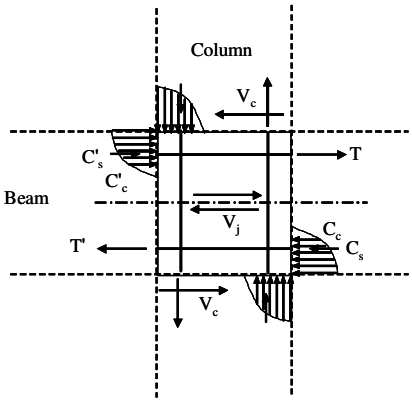

Figure 1. Horizontal shear force in joint core.

equilibrate moments acted by framing beams. Concurrently, the longitudinal beam bar in the joint is also subject to a large bond stress. As a result, the joint commonly fails by either joint shear or bar pull-out failure.

Among the experimental results of beam-column joints reported so far, the experimental works of non-seismically detailed reinforced concrete beam-column joints were still limited (Hegger *et al.*, 2003, Li and Pan, 2002, Park, 2002, Supaviriyakit *et al.*, 2006) Research in this area is still needed to form a database for building retrofitting and strengthening. In contrast to other experimental works, in which researchers presumed parameters influencing joint behavior, such as reinforcement ratio, material strength, confining hoops, column size, etc., in their experiments, this research puts more emphasis on actual existing structures. By collecting structural data and reinforcing details of existing reinforced concrete buildings, the authors defined structural and geometrical indices. Based on these indices, specimens were grouped according to the column tributary area and constructed to represent the buildings in each category.

2. Geometrical and structural indices of existing buildings

The authors conducted the reversed cyclic test of three half-scale non-ductile interior beam-column joint specimens. In the past, the parameters chosen by researchers were reinforcement ratios, amount of joint confinement reinforcements, material strengths, member sizes, etc (CEB, 1996). In this research, however, instead of presuming parameters affecting beam-column joint behavior, the authors attempted to design the specimens that could represent the actual existing buildings as close to possible. First, we collected and investigated ten existing buildings to obtain the key practical structural parameters that characterized these buildings. The specimens were constructed to have the indices close to the actual ones. The specimen fabrication and reinforcing details were also made as close as the actual construction as possible. The governing parameter chosen in this study was the column tributary area. According to the investigated data, there were certain correlations between structural and geometrical indices and column tributary area, hence, it was appropriate to select column tributary area as a studied parameter.

A database of ten reinforced concrete mid-rise buildings in Bangkok was gathered. All buildings were reinforced concrete beam-column frame without shear wall and had 5-15 stories. The types of buildings covered essential facilities, including universities, schools, apartments and hospitals as shown in Table 1. These buildings were designed according to the non-seismic provisions of the ACI building code (2005) considering only gravity load. Since buildings were designed in accordance with the ACI code, the experimental findings are probably applicable not only to buildings in Thailand, but also to buildings designed and detailed according to the ACI code in general.

The buildings were grouped into three categories based on column tributary area (Figure 2(a)), as buildings with large, medium, and small column tributary area. Based on the collected data, the area range was set to 40-48 m^2, 20-30 m^2, and 9-18 m^2 for the large, medium, and small category, respectively. In order to characterize the structural behavior of beam-column connections, the structural and geometrical indices were defined for beam, column, and beam-column joint. The structural indices of beam included tension and

Table 1. Database of investigated buildings

No.	Code Name Building	Type of of Story	Number Height(m)	Clear Story Length (m)	Span	Column size Tributary Area (m^2)	Approximate	Remark
1	9UNI-1	University	9	4.0	8.0	600x800	48.0	JL
2	9UNI-2	University	9	4.2	7.0	800x800	57.0	JL
3	21OFF-3	Office	21	4.5	9.0	1200x1200	40.5	JL
4	12Hos-4	Hospital	12	4.5	5.0	600x600	29.5	JM
5	12AP-5	Apartment	12	3.0	8.0	400x1200	32.4	JM
6	9SCL-6	School	9	4.0	7.0	500x800	24.0	JM
7	15AP-7	Apartment	15	3.2	4.3	400x800	20.0	JM
8	12OFF-8	Office	12	4.5	6.2	700x700	17.5	JS
9	9Ap-9	Apartment	9	2.7	3.0	200x400	9.0	JS
10	9AP-10	Apartment	9	2.5	3.4	300x500	13.7	JS

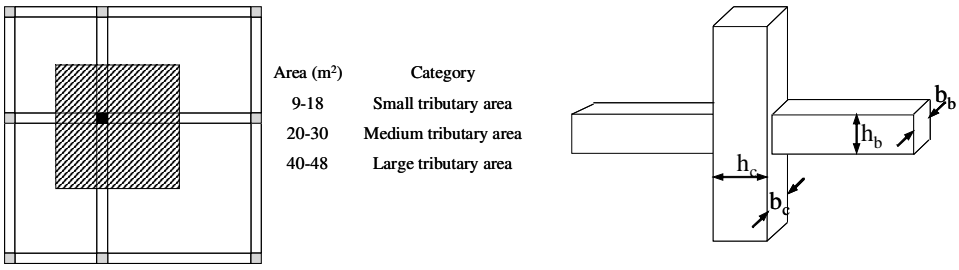

(a) Definition of column tributary area (b) Joint dimensions

Figure 2. Definition of column tributary area and joint dimensions

compression reinforcement ratio, shear span-to-depth ratio, flexural capacity-to-shear capacity ratio, and transverse reinforcement ratio. The structural and geometrical indices of column included axial force ratio, shear span-to-depth ratio, flexural capacity-to-shear capacity ratio, longitudinal reinforcement ratio, and transverse reinforcement ratio. The structural and geometrical indices of beam-column joint included column depth-to-bar diameter ratio, column width-to-beam width ratio, column depth-to-beam depth ratio, confinement reinforcement index, column flexural capacity-to-beam flexural capacity ratio, and joint shear-to-joint shear strength ratio. Figure 2(b) illustrates the definition of joint dimensions used to calculate these indices.

The structural and geometrical indices were calculated for the beam-column joint of buildings in each category. The range of indices is shown in Table 2-4. It is noted that none of buildings had stirrups in the joint. The column longitudinal bars were usually spliced just above the joint with lap length of 350 mm. It is noted that almost all buildings had column stronger than beam. This complies with the strong column weak beam concept despite no capacity design was applied in the design of these buildings. The ratio of column depth to bar diameter ratio (h_c/d_b) of all buildings were greater than 20, which was the minimum requirement of the ACI code (2005) for frames in high seismic zones. The significant feature is the size of column, which depends on the column tributary area. There is a tendency of increasing column size with increasing tributary area. As the column size gets larger, the bond demand represented by the bond index ($BI = f_y d_b / 2h_c\sqrt{f'_c}$) of the longitudinal bar decreased, the joint shear to joint shear capacity ratio is lowered, and the nominal column to beam moment capacity increased.

3. Test specimens

Based on the investigated structural and geometrical indices, three half-sized beam-column specimens, namely, JL, JM, and JS were constructed to represent buildings with large, medium, and small column tributary area, respectively. The indices of these specimens were designed to be as close as possible to the mean values calculated from the actual building in each category as shown in Table 2-4. The specimen dimensions and reinforcement details are illustrated in Figures 3-4. The size of the column in the direction of loading is 400, 350, and 300 mm, respectively. However, the beam depth was kept constant in all three specimens to keep the ratio of beam height to column height close to the collected data as shown in Table 2-4. The 12-mm diameter reinforcing bar was used as a longitudinal reinforcement in beam and column. The average tested yield and tensile strengths of the bar were 499 and 615 MPa, respectively. The 3-mm diameter plain mild steel bar was used as a transverse reinforcement in beam and column. The tested yield and tensile strengths of the bar were 291 and 339 MPa, respectively. The average tested compressive strength of a standard concrete cylinder at 28 days was 26.7 MPa.

4. Test set-up and boundary condition

The test set-up and boundary conditions are shown in Figure 5. The lateral forced displacement was applied at the top of the column through a 500 kN hydraulic actuator. The ends of the beam were supported by rollers that allowed free horizontal movement to simulate lateral drift. The bottom end of the column was supported by a hinge which allowed no movement in any direction. The axial load of

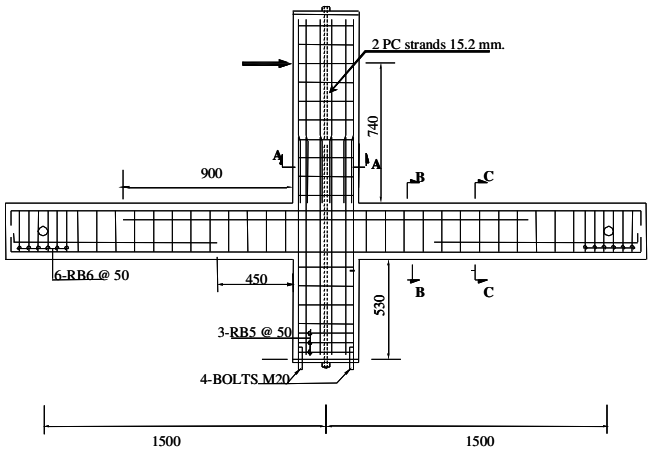

Figure 3. Geometry, dimension and reinforcement of all specimens (unit:mm)

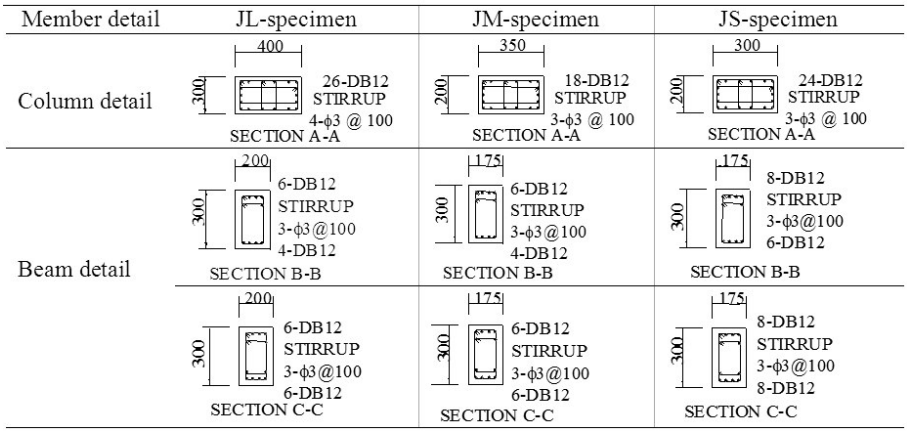

Figure 4. Cross section of beams and columns (unit: mm)

Table 2. Structural indices for buildings with large tributary area

No.	Code	Clear story Height (m)	BI	$\frac{h_c}{d_b}$	$\frac{b_b}{b_c}$	$\frac{h_b}{h_c}$	$\frac{M_{nc}}{M_{nb}}$	$\frac{V}{V_n}$	$\frac{\rho_{sv} f_y}{f_c'}$
1	9UNI-1	4.0	4.30	32	0.417	0.750	3.442	1.126	0.0
9	9UNI-2	4.2	4.81	29	0.625	1.000	2.098	0.972	0.0
10	21-OFF-3	4.5	3.09	48	0.417	0.667	5.047	0.911	0.0
Maximum		4.5	4.81	48	0.625	1.000	5.047	1.126	0 .0
Minimum		4.0	3.09	29	0.417	0.667	2.098	0.911	0 .0
Average		4.2	4.07	36	0.486	0.806	3.529	1.003	0.0
Std. Dev.		0.3	0.88	10	0.120	0.173	1.477	0.111	0.0
Specimen JL			4.45	33	0.667	0.750	3.049	0.903	0.0

Table 3. Structural indices for buildings with medium tributary area

No.	Code	Clear story Height (m)	BI	$\frac{h_c}{d_b}$	$\frac{b_b}{b_c}$	$\frac{h_b}{h_c}$	$\frac{M_{nc}}{M_{nb}}$	$\frac{V}{V_n}$	$\frac{\rho_{sv} f_y}{f_c'}$
4	12Hos-4	4.5	6.19	24	0.500	1.083	2.372	0.912	0.0
5	12AP-5	3	2.24	60	0.750	0.667	3.403	1.029	0.0
6	9SCL-6	4	4.96	32	0.700	1.000	1.538	1.115	0.0
7	15AP-7	3.2	4.64	32	0.750	0.625	2.127	1.172	0.0
Maximum		4.5	6.19	60	0.750	1.083	3.403	1.172	0 .0
Minimum		3.0	2.24	24	0.500	0.625	1.538	0.912	0 .0
Average		3.7	4.51	37	0.675	0.844	2.360	1.057	0.0
Std. Dev.		0.7	1.65	16	0.119	0.232	0.779	0.113	0.0
Specimen JM			5.09	29	0.875	0.857	1.682	1.382	0.0

12.5% of column axial capacity was applied to the column by means of vertical prestressing. The column was pushed forward and pulled backward in a reversed cyclic. The load type was quasi-static with the load application rate of half an hour to complete one cycle. The lateral drift ratio, defined as the ratio of the lateral displacement at the top of the column to the column height, was incrementally applied at 0.25%, 0.50%, 0.75%… as shown in Figure 6. The target loop was repeated twice for each drift level. The load was continued until and beyond the peak load to trace the post-peak behav-

Table 4. Structural indices for buildings with small tributary area

No.	Code	Clear story Height (m)	BI	$\frac{h_c}{d_b}$	$\frac{b_b}{b_c}$	$\frac{h_b}{h_c}$	$\frac{M_{nc}}{M_{nb}}$	$\frac{V}{V_n}$	$\frac{\rho_{sv} f_y}{f_c'}$
8	12OFF-8	4.5	5.94	25	0.571	1.143	0.732	2.668	0.0
9	9Ap-9	2.7	5.90	25	1.000	1.000	2.331	1.677	0.0
10	9AP-10	2.5	8.57	20	0.833	0.900	1.473	3.504	0.0
Maximum		4.5	8.57	25	1.000	1.143	2.331	3.504	0 .0
Minimum		2.5	5.90	20	0.571	0.900	0.732	1.677	0 .0
Average		3.2	6.80	23	0.802	1.014	1.512	2.616	0.0
Std. Dev.		1.1	1.53	3	0.216	0.122	0.800	0.915	0.0
Specimen JS			5.94	25	0.875	1.000	1.187	2.282	0.0

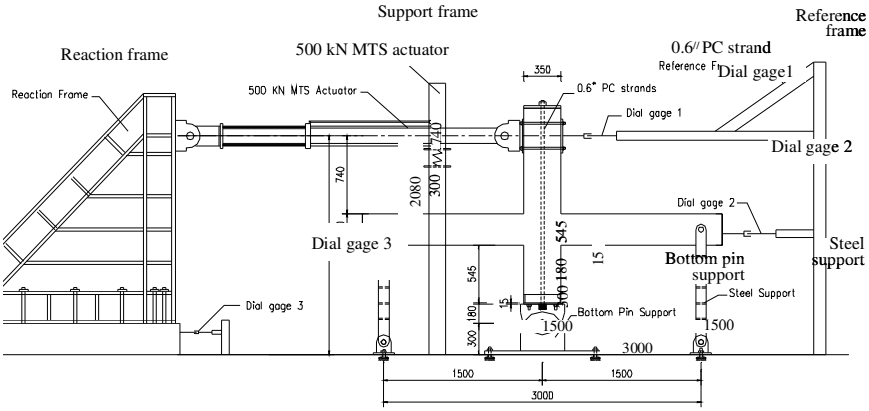

Figure 5. Test set-up

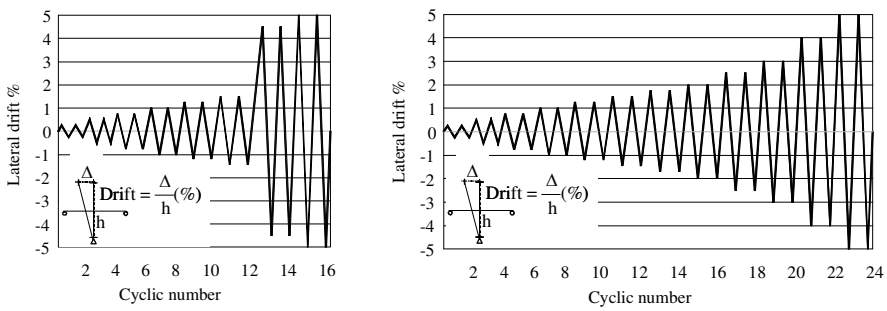

(a) JL- Specimen (b) JM and JS-Specimen

Figure 6. Displacement history of each specimen

ior. The measurements included forces, displacements, and strains at various locations of the specimens.

5. Test Results and Discussions

5.1 General observation, cracking process and failure mode

Specimen JL showed first flexural cracks in the beam during 0-0.25% drift ratio. The behavior was elastic during these initial drifts as shown in Figure 7(a). The flexural cracks grew in size and number as the drift ratio increased. The beam yielded at 1.0% drift. The first diagonal crack at the joint was observed at 1.25% drift. Bond splitting cracks were also observed at the longitudinal steel level. The beam maintained yielding up to 4.6% drift when substantial crushing of concrete at the beam compression zone took place and spalled off, exposing beam bars as shown in Figure 8(a). The specimen lost it's strength abruptly. Throughout the entire loading, no cracks were observed in the column lap

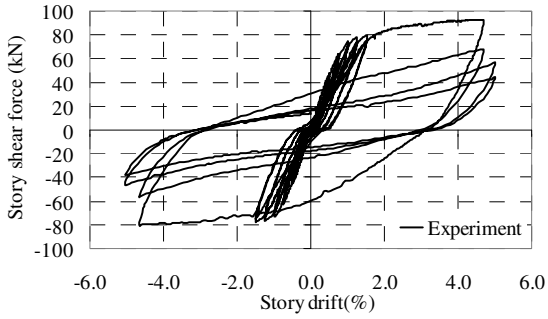

(a) Specimen JL

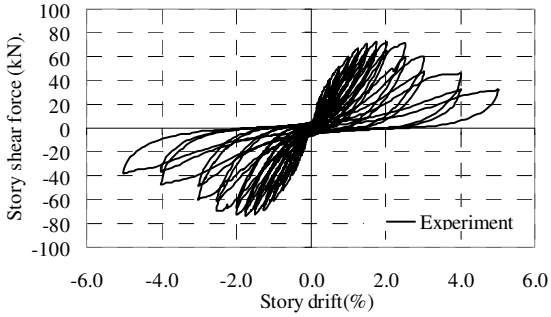

(b) Specimen JM

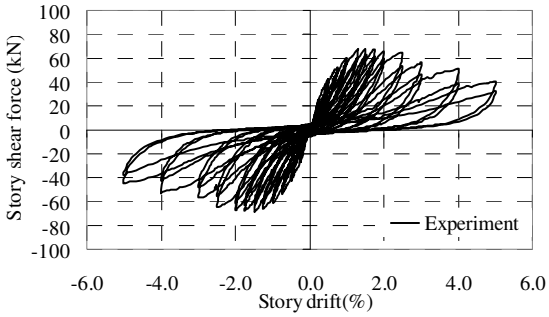

(c) Specimen JS

Figure 7. Relationship between applied load and displacement of each specimen

splice region above the joint. No damage was observed in the joint except some few joint shear cracks. The failure of the beam was classified as ductile flexural failure. The hysetersis loops were wide, indicating large energy dissipation in bending mode. It is noted that even though the specimen lacked ductile reinforcement details and was not designed to resist seismic load, it could perform fairly well. The good performance was supposedly attributed to the size of column which was comparatively large, in order to support large gravity load for the large tributary area. As the column size is large, the joint shear stress has decreased naturally, and the bond demand of the column lap splice is relieved. The bending failure then occurred in the beam according to strong column weak beam principle. This experiment demonstrated that the performance of beam-column joint was satisfactory, when the column size was large even without ductile reinforcement details. However, the ductility can be enhanced by providing closed stirrups near the beam's end to prevent concrete spalling and reinforcement buckling.

The behavior of JM and JS was similar, hence they are discussed together. The flexural cracks were observed in the beam in the beginning of the 0-0.25% drift ratio (Figures 7(b), 7(c)). The first diagonal crack was found in the joint core at 0.5% drift ratio. They formed an X-pattern following the alternate load directions. The flexural cracks in beams and the diagonal cracks in joint cores continued to grow in size and number until the specimen reached the peak load of 72 kN at 1.75% drift ratio for specimen JM, and 68 kN at 1.5% drift ratio for specimen JS. After this cycle, no new cracks were found in the beam, but diagonal cracks continued to widen in the joint core. This was followed by spalling of concrete at the center of the joint area. At 3% drift, the concrete spalling extended throughout a wider area of the joint, exposing column longitudinal bars. The test was continued until 5% drift ratio, where concrete spalling covered

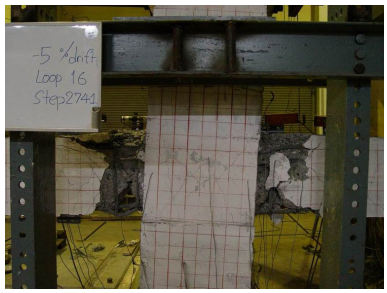

(a) Failure of specimen JL

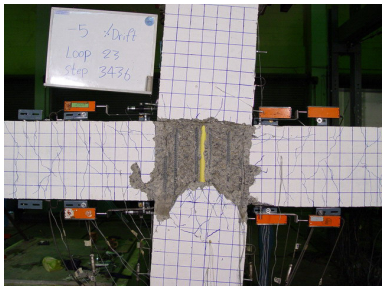

(b) Failure of specimen JM

(c) Failure of specimen JS

Figure 8. Failure of specimen

the entire joint area (Figures 8(b), 8(c)) and extended into the column above and below the joint. The failure mode of JM and JS could be classified as joint shear failure. It should be noted that no damage was observed at the column bar splice region above the joint. The joint shear failure is not desirable as it is abrupt and results in pinched hysteresis loops with low energy dissipation. The experiment indicated the vulnerability of existing buildings with small column tributary area. Future research should look into the retrofitting of these classes of buildings.

5.2 Force-joint shear deformation relation

To gain an insight into the behavior of each specimen, local deformations and strains were measured at critical regions of the specimens. The force-shear deformation in the joint zone is compared among three specimens in Figure 9. The joint shear deformation was plotted in terms of shear angle. Specimen JL showed clearly smaller joint shear deformation compared with JM and JS. The maximum values of shear deformation at failure were 0.00012, 0.02 and 0.015 radian in JL, JM and JS, respectively. These shear deformation values correlated well with observed damage level in the joint of each specimen. Little shear inelasticity was observed in JL, while substantial damage existed in joints of specimen JM and JS. On the other hand, the hysteresis force versus shear deformation of JM and JS showed severe pinching, which partly accounted for the pinching of the global load displacement relation.

6. Force-steel strain relation

The force and strain relations of bottom bars located 50 mm away from the joint face (STBBR-gage) and at the middle of the joint (STBBM-gage) are plotted in Figures 10 and 11. Specimen JL reached yielding and developed large plastic strain, while JM and JS merely reached yielding without developing high plasticity. In each specimen, the

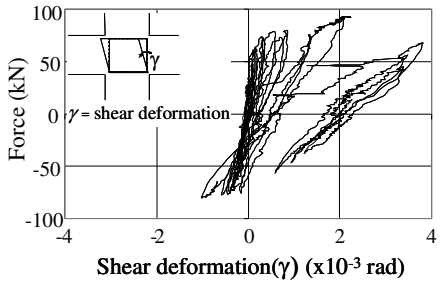

(a)Specimen JL

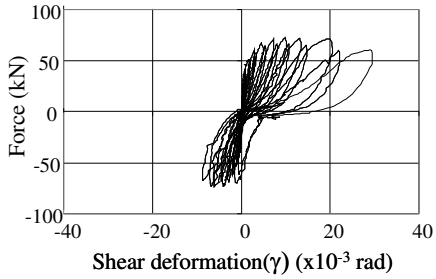

(b) Specimen JM

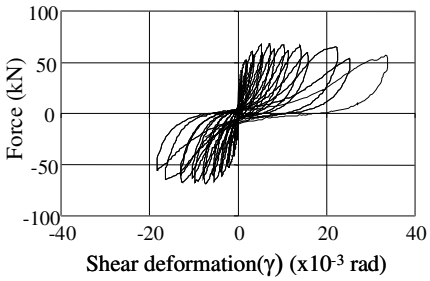

(c) Specimen JS

Figure 9. Force- joint shear deformation relationship of each specimen

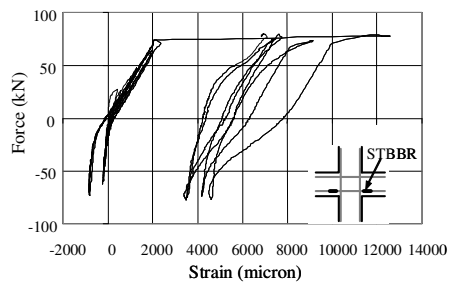

(a)Specimen JL

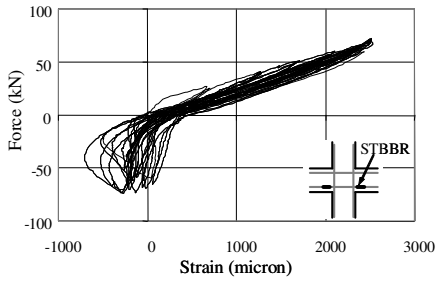

(b) Specimen JM

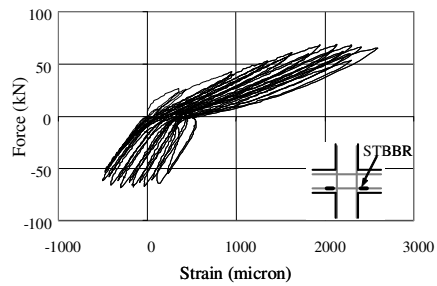

(c) Specimen JS

Figure 10. Strain of bottom beam bar (STBBR) at 50 mm away from the joint face

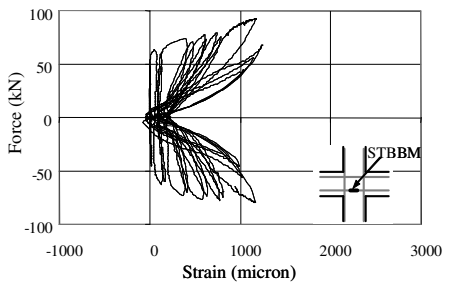

(a)Specimen JL

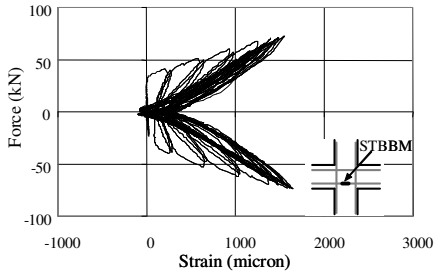

(b) Specimen JM

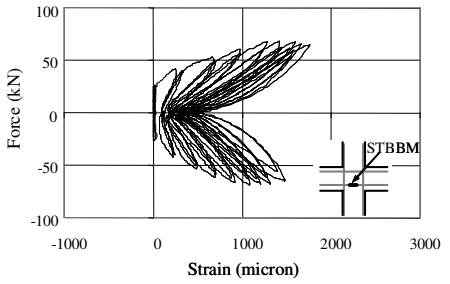

(c) Specimen JS

Figure 11. Strain of bottom beam bar (STBBM) at the middle of joint

strains of bottom beam bars at 50 mm from the joint face and at the middle of the joint showed obviously different behaviors. At 50 mm from the joint face, the steel bar of JL was subject to alternate compressive and tensile strains in the early drift levels. But the strains turned into purely tensile at high drift levels regardless of the loading direction. As for JM and JS, the strain behavior on the tensile and compressive sides was obviously unsymmetrical. This is due to the fact that the strain of the steel bar was smaller on the compressive than on the tensile side. With increasing drift ratio, the tensile strain continuously increased, whereas the compressive strain (negative strain value) initially increased, but gradually decreased later. This behavior was dealt with by the interface pull-out crack, which was caused by local bond deterioration, and had taken place in the previous opposite load direction. During reverse loading, the pull-out crack was not completely closed, thus, a positive strain value still remained in steel, and was accumulated in subsequent cycles. The steel on the compression side became positive instead of negative.

The behavior of the steel bar at the middle of the joint showed a butterfly pattern. The strains on the compression and tension side were symmetrical at about zero force level. The steel strain at the middle of the joint of all specimens was always tensile regardless of the load direction. Furthermore, it should be noted that strains at the middle of the joint were approximately equal in all specimens, and that the magnitude was less than the yield strain. As seen for all specimens, the yielding did not spread deep into middle of the joint. This was contrasted with the value at 50 mm away the column face, especially for the steel strain in JL. This indicated that the bond within joint core was not completely lost along the length of the bar. The variations of strain with load cycles are plotted in Figures 12(a)-12(c). Specimen JL maintained bond conditions quite well before yielding at 1.25% drift ratio. After yielding, the bar strain was purely tensile, indicating the local loss of bond at the section with high strain value. For Specimen JM and JS, the local bond was lost in the early 0.75% drift.

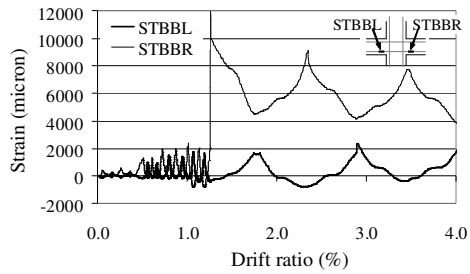

(a)Specimen JL

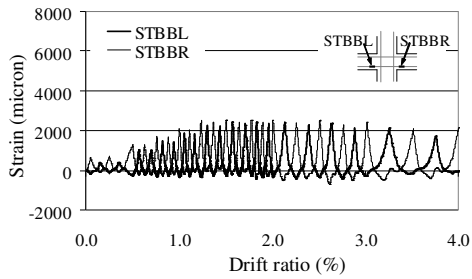

(b) Specimen JM

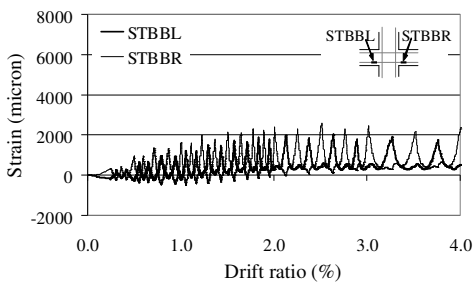

(c) Specimen JS

Figure 12. Strain history of bottom beam bar at 50 mm away from the joint fac

The bond demand of longitudinal beam bar was associated with the ratio of column depth to bar diameter (h_c/d_b). According to the ACI code, this ratio is required to be not lower than 20 for frames in high seismic zones. The h_c/d_b ratios of JL, JM, and JS were 33, 29, and 25, respectively. Therefore, the bond demand of JS seemed to be more severe than of JM and JL, because the size of the column was smaller. In view of the experimental results, no entire loss of bond was observed in any specimen. But, the local loss of bond at the beam section close to the joint could not be avoided in all specimens. This local bond loss was associated with pull-out slip of beam bars.

7. Conclusion

This paper presented the reversed cyclic test of non-ductile designed interior RC beam-column joints typical for constructions in low to moderate seismic zones. According to the evaluation of ten old existing RC beam-column frame buildings, there existed some correlations among key structural and geometrical indices and the column tributary area. With increasing tributary area, the trend indicated larger column size, lower bond demand, lower joint shear stress, and higher column flexural capacity. The experimental results showed that specimens with small to medium column tributary area were vulnerable to brittle joint shear failure, while specimen with large column tributary area could achieve moderately ductile yielding, even though the ductile reinforcement detailing was not provided. The strain measurements of longitudinal steels indicated local bond deterioration of steel bars at the column face in all specimens, but the bond deterioration did not spread in to the center of the joint core. No entire loss of bond was observed in all specimens. But the local bond pull-out was observed in all specimens, although all satisfied the minimum ACI column depth to bar diameter ratio of 20. The source of severe pinching in hysteresis loops was derived from the bond pull-out and joint shear distress.

Acknowledgements

The authors are very grateful to the Thailand Research Fund (TRF) for providing the research fund RMU4880022 to carry out the research.

References

ACI committee 318. 2005. Building Code Requirements for Structural Concrete and Commentary, Michigan

Aycardi, L.E., Mander, J.B. and Reinhorn, A.M. 1994. Seismic resistance of reinforced concrete frame structure designed only for gravity loads: Experimental performance of subassemblages, ACI Structural Journal, 91(5): 552-563

Bracci, J.M., Reinhorn, A.M. and Mander, J.B. 1995. Seismic resistance of reinforced concrete frame structure designed only for gravity loads: Performance of Structure system, ACI Structural Journal, 92(5): 597-609

CEB State of the Art Report. 1996. RC frames under earthquake loading, Thomas Telford, London

El-attar, A.G., White, R.N., and Gergeley, P. 1997. Behavior of gravity load designed reinforced concrete buildings subjected to earthquakes, ACI Structural Journal, 94(2):133-145.

Hakuto, S., Park, R., and Tanaka, H. 2000. Seismic load tests on interior and exterior beam-column joints with substandard reinforcing details, ACI Structural Journal, 97(1): 11-25.

Hegger, J., Sherif, A. and Roeser, W. 2003. Nonseismic design of beam-column joint. ACI Structural Journal, 100(5): 654-664.

Li, B. and Pan, T.C. 2004. Seismic performance of reinforced concrete frames under low intensity earthquake effects, Proceedings of the 13th World Conference on Earthquake Engineering, Vancouver

Li, B., Wu, Y. and Pan, T.C. 2002. Seismic behavior of non-seismically detailed interior wide beam-column joints-Part I: Experimental results and observed behaviors, ACI Structural Journal, 99(6): 791-802.

Maekawa, K., Pimanmas, A. and Okamura, H. 2003. Nonlinear mechanics of reinforced concrete, Spon Press, London.

Park, R. 2002. A Summary of Results of Simulated Seismic Load Tests on Reinforced Concrete Beam-Column Joints, Beams and Columns with Substandard Reinforcing Details. Journal of Earthquake Engineering, No 6: 147-174

Riggs, H., and Powell, G. 1986. Rough crack model for analysis of concrete, ASCE J. Eng. Mech, 112(5): 448-464

Supaviriyakit, T., Pimanmas, A. and Warnitchai, P. 2006. Effect of removing initial bond between beam bar and concrete on cyclic response of non-ductile beam-column joint, Proceeding of 10th East Asia-Pacific Conference on Structural engineering and construction, Thailand.

Vecchio, F.J., and Collins, M.P. 1986. The modified compression field theory for reinforced concrete elements subjected to shear, ACI Structural Journal, 83(2): 219-231.

Vecchio, F.J., and Collins, M.P. 1988. Predicting the response of reinforced concrete beams subjected to shear using the modified compression field theory, ACI Structural Journal, 85(4): 258-268.

Warnitchai, P. 2004. Development of seismic design requirements for buildings in Bangkok against the effects of distant large earthquakes, Proceedings of the 13th World Conference on Earthquake Engineering, Vancouver

Notation

b_b beam width

b_c column width

d_b diameter of longitudinal beam bar

h_b beam depth

h_c column depth

E_s elastic modulus of steel bar

f_c' cylindrical compressive strength of concrete

f_y yield strength of reinforcement

M_{nc} nominal column flexural capacity

M_{nb} nominal beam flexural capacity

V joint shear force

V_n joint shear strength

ρ_{sv} volumetric ratio of confinement reinforcement

BI bond index (BI = $f_y d_b / 2h_c \sqrt{f_c'}$)